

Effects of longer-range interactions on unconventional superconductivity

S. Raghu,^{1,2} E. Berg,³ A. V. Chubukov,⁴ and S. A. Kivelson¹

¹*Department of Physics, Stanford University, Stanford, California 94305, USA*

²*Stanford Institute for Materials and Energy Science, SLAC National Accelerator Laboratory, Menlo Park, California 94025, USA*

³*Department of Physics, Harvard University, Cambridge, Massachusetts 02138, USA*

⁴*Department of Physics, University of Wisconsin, Madison, Wisconsin 53706, USA*

(Received 24 November 2011; revised manuscript received 28 December 2011; published 9 January 2012)

We analyze the effect of the nonvanishing range of electron-electron repulsion on the mechanism of unconventional superconductivity. We present asymptotically exact weak-coupling results for dilute electrons in the continuum and for the 2D extended Hubbard model, as well as density-matrix renormalization group results for the two-leg extended Hubbard model at intermediate couplings, and approximate results for the case of realistically screened Coulomb interactions. We show that T_c is generally suppressed in some pairing channels as longer range interactions increase in strength, but superconductivity is not destroyed. Our results confirm that electron-electron interaction can lead to unconventional superconductivity under physically realistic circumstances.

DOI: [10.1103/PhysRevB.85.024516](https://doi.org/10.1103/PhysRevB.85.024516)

PACS number(s): 74.20.-z, 74.20.Mn, 74.20.Rp, 74.25.Dw

I. INTRODUCTION

That unconventional superconductivity can arise in models with short-ranged repulsive interactions between fermions has been known for some time, beginning with the pioneering work by Kohn and Luttinger.¹ This issue has been revisited multiple times in the last few decades, since the discovery of unconventional superconductivity in the cuprates. For the Hubbard model with local repulsion U and fermionic bandwidth W , the existence of superconductivity in p -, d -, f -, or g -wave, as well as sign-changing s -wave, channels has been established from asymptotic weak-coupling analysis in the limit $U/W \ll 1$ in two and three dimensions,²⁻⁸ from the observation of a positive pair-binding energy computed from exact diagonalization on various “Hubbard molecules,”⁹ from dynamical cluster approximation (DCA)¹⁰ and cluster dynamical mean-field theory (DMFT) calculations,¹¹ and from extensive density-matrix renormalization group (DMRG) studies^{12,13} of various ladder systems extrapolated to the thermodynamic limit.

While there is still some controversy over the strength of the pairing tendencies under particular circumstances, there is a growing consensus that superconductivity in the repulsive Hubbard model is generic under a wide range of circumstances. Various physically motivated approximate calculations, including numerically implemented functional renormalization group (FRG),¹⁴ dynamical cluster approximation (DCA)¹⁰ and cluster dynamical mean-field theory (DMFT) calculations,¹¹ fluctuation exchange approximation (FLEX),¹⁵ Eliashberg,¹⁶ and self-consistent two-particle calculations,¹⁷ as well as strong-coupling approaches based on variational wave functions¹⁸ and slave-particle mean-field theories,^{19,20} have also strongly indicated that such unconventional pairing is present, especially near half filling, and that T_c is maximized in the physically relevant range of intermediate coupling, $U \sim W$, and decreases at both larger and smaller U . The decrease of T_c at smaller U is due to the fact that the strength of any induced attractive interaction must vanish as $U \rightarrow 0$, while the decrease as $U \rightarrow \infty$ is due to Mott physics which tends to localize fermions near particular

lattice sites,^{20,21} potentially suppressing both the superfluid stiffness²² and the pairing tendencies²³ of the electrons.

It is broadly (although not universally²⁴) accepted that the basic features of superconductivity arising from short-range repulsion between electrons are moderately generic and must be in play in a broad class of unconventional superconductors such as the cuprates, heavy-fermion and organic superconductors, Sr_2RuO_4 , and the recently discovered Fe pnictides, despite differences in band structure and local quantum chemistry.²⁵ In particular, estimates of the optimal T_c for d -wave pairing in 2D Hubbard models, obtained using a variety of approximate computational approaches,^{10,11,13,15-18,26} suggest that $\text{Max}[T_c] \sim 10^{-2} v_F/a_0$, where v_F is the Fermi velocity averaged over the Fermi surface (FS) and a_0 is the interatomic distance. Using $v_F/a \sim 1$ eV,²⁷ one obtains an estimate of the optimal T_c of order 100 K, comparable to the d -wave transition temperatures found in optimally doped cuprates.

However, in addition to the vexing problem of how to unambiguously establish or falsify the applicability of a particular electronic pairing mechanism to real materials, at least one key theoretical question remains to be addressed: It is well known that longer-ranged components of the electron-electron interaction, even simply a nearest-neighbor repulsion V between electrons, suppress the pairing tendencies of the Hubbard model. As we will discuss below, this can be seen clearly from the structure of the asymptotic weak-coupling approach and also in exact diagonalization studies of Hubbard molecules. This effect has also been investigated in DMRG studies of t - J ladders²⁸ (which we extend to Hubbard ladders in the present paper). Thus, the issue to be addressed is whether the deleterious effects of longer-range components of the electron-electron repulsion make a purely electronic mechanism of superconducting pairing physically implausible.

The physics behind the suppression of T_c is transparent: An effective attraction which can give rise to unconventional superconductivity in p -wave, d -wave, extended s -wave, and other channels emerges in the theory from the renormalization

(screening) of the local repulsive interaction U by particle-hole fluctuations of the continuum of fermions. For small U , the induced interactions are necessarily of order U^2/W or smaller, and more generally one expects the induced interactions to be overall weaker than the bare interactions that give rise to them. However, if the bare interaction is short ranged, then it only contributes in the trivial s -wave channel, while because the polarization of the particle-hole continuum depends on the energy and momentum transfer between initial and scattered fermions, the induced interactions are nonlocal and may have attractive contributions in other pairing channels.

If, however, the bare interaction is extended, so it contributes a repulsive piece in the same extended s -wave, p -wave, d -wave, etc., channels, the competition between the bare and induced interactions becomes more serious. This issue has been recently addressed in a particularly pointed fashion by Alexandrov and Kabanov (AK) (Ref. 29). They have concluded that in models with a screened Coulomb interaction, the bare repulsion in non- s -wave channels is so significant that it effectively overwhelms the induced attractions, thus eliminating as physically realistic the entire class of theories in which the pairing comes from electron-electron repulsion.

We will show that the conclusion of Ref. 29 is not warranted. From the exact diagonalization and DMRG studies discussed below, it is clear that there is no anomalous sensitivity of the pairing strength to longer-range interactions; in an extended Hubbard model, significant suppression of unconventional pairing occurs only when the farther neighbor interactions, V , are a noticeable fraction of U , and not when they exceed the (much smaller) gap scale associated with pairing. From the various approximate extensions of the weak-coupling analysis to intermediate coupling, it is clear that a key physical ingredient missed in the discussion of AK is the near resonant enhancement of the induced attractions at special favored wave vectors when the system is in (not too close) proximity of a density wave ordering transition; under these circumstance, if the favored vectors appropriately nest the FS, the appropriate weighted average of the bare and induced interactions can favor unconventional superconductivity, despite the fact that the induced interactions are generically weaker than the bare interactions.³⁰⁻³²

Even in the strictly weak-coupling limit, where controlled calculations can be carried through (as shown below), the effect of longer-range interactions turns out to be surprisingly muted. Longer-ranged interactions in lattice models (interactions between nearest neighbors, second-nearest neighbors, etc.) generally have components only in some particular pairing channels and do not contribute to other channels. On the other hand, the particle-hole polarization bubbles which enter the induced interactions have components in all channels, and quite often more than one component is attractive. In this situation, it is quite possible that longer-range interaction either does not affect the leading pairing component at all, or it suppresses the leading attractive component but leaves the subleading one unaffected.

In this context, we revisit in this paper the issue of unconventional superconductivity from electron-electron repulsion in an extended Hubbard model on a square lattice with an on-site repulsion of magnitude U and nearest-neighbor and next-nearest-neighbor couplings of magnitudes V and V' ,

respectively. We study this problem using the same asymptotic weak-coupling methods that were previously applied to the pure Hubbard model, complemented by a new DMRG study of a two-leg ladder. We consider arbitrary fermionic density and analyze the pairing problem for various relations between V, V', U , and the bandwidth W . It is important to stress that the physics governing U and V is generally quite distinct, and they should be considered as essentially independent parameters. For instance, in a transition-metal oxide, U reflects the atomic physics at short distances, while V reflects the screening effects of all the degrees of freedom that are integrated out at high energies, including the polarization of the surrounding medium in the solid-state environment.

We find that the interplay between the short- and longer-range repulsive interactions results in a fascinating, complex phase diagram with a large number of distinct unconventional superconducting phases. The longer-range interactions do indeed tend to suppress unconventional superconductivity in some channels, but still we find that unconventional superconductivity emerges for all densities and for all relations between parameters of the model.

This paper is organized as follows. In the next section, we review the weak-coupling approach to pairing in a system of fermions with generic finite-range interactions. In Sec. III we discuss the case of short-range interactions and small electron density, where the fermionic dispersion can be approximated by a parabola. In Sec. IV we extend the approach to arbitrary electron densities and analyze the extended Hubbard model with nearest- and next-nearest-neighbor interactions. In Sec. V we consider the case of screened Coulomb interactions, which we can only treat approximately, even in the small r_s limit. In Sec. VI, we present the results of the DMRG calculations of the pairing amplitudes in Hubbard ladders. We discuss the results and present our conclusions in Sec. VII.

II. ASYMPTOTICALLY EXACT WEAK-COUPLING APPROACH

The basic idea of the Kohn-Luttinger (KL) approach to superconductivity is that the pairing interaction is given by the irreducible vertex in the particle-particle channel, which is generally different from the bare interaction between the two given fermions and includes contributions from the continuum of particle-hole excitations. These additional contributions to the pairing interaction can give rise to an attraction in a particular pairing channel even if the original interaction between two fermions is uniformly repulsive.

The KL approach can be formally justified if there is a separation of scales: Superconductivity is assumed to come from fermionic states very near the FS, while the renormalization of the irreducible pairing interaction comes from fermions with energies comparable to the Fermi energy. In this situation the fully renormalized pairing interaction can be approximated by its value when both incoming and outgoing fermions are on the FS and the two incoming fermions have opposite momenta and zero energy (where the energy is measured as deviation from the chemical potential). Such a separation of scales clearly occurs when the interaction U is much smaller than the fermionic bandwidth W ; under appropriate circumstances,

it may hold approximately (in a physical sense) even when U is comparable to the bandwidth.¹⁶

The KL approach can be implemented in terms of a two-step renormalization group (RG) procedure:⁸ In the first step, we integrate out all modes outside a narrow range of energies Ω_0 about the Fermi energy. Ω_0 is not a physical energy in the problem, but rather a calculational device. It is chosen large enough so that the interactions can be treated perturbatively (e.g., the Cooper logarithms are still small), but small enough that it can be set to zero in all renormalizations in nonsingular channels without causing significant error; i.e., it is chosen to satisfy the inequalities

$$N_F U^2 \gg \Omega_0 \gg E_F \exp\{-1/(N_F U)\}, \quad (1)$$

where N_F is the density of states (DOS) at the Fermi energy (for both spin orientations) and E_F is the Fermi energy. The effective interactions generated in the process then serve as input interactions in a second step, in which the remaining problem is solved using the logarithmical RG technique,^{33,34} which is equivalent to BCS when only the pairing channels are singular. (It involves a more complex parquet RG if some other channel, e.g., SDW or CDW, is also singular and competes with superconductivity,^{30,34} a situation we will not consider explicitly for the present.) T_c is, up to a multiplicative constant, given by the energy scale T^* at which the pairing interaction grows to be of order one. It was shown by explicit perturbative calculation of T_c up to fourth order in U that the resulting expression for T^* is independent of Ω_0 (Refs. 8,35). The generic prescription for computing the leading-order asymptotic behavior of T_c for weak interactions is the following:⁸ First, compute the effective interaction in the Cooper channel at energy scale Ω_0 perturbatively, to second order in the bare interaction. The corresponding diagrams are shown in Fig. 1. We denote this effective interaction as $\Gamma^{(a)}(\mathbf{k}, -\mathbf{k}; \mathbf{p}, -\mathbf{p}) = \Gamma^{(a)}(\mathbf{k}, \mathbf{p})$, where \mathbf{k} and \mathbf{p} denote points on the FS and the superscript a differentiates between whether the electron pair forms a spin singlet ($\Gamma^{(s)}$) or a spin triplet ($\Gamma^{(t)}$). We then construct the related dimensionless matrix

$$\gamma^{(a)}(\mathbf{k}, \mathbf{p}) \equiv \bar{N}_F \sqrt{\bar{v}_F/v_F(\mathbf{k})} \Gamma^{(a)}(\mathbf{k}, \mathbf{p}) \sqrt{\bar{v}_F/v_F(\mathbf{p})}, \quad (2)$$

where $v_F(\mathbf{k})$ is the magnitude of the Fermi velocity at a given point \mathbf{k} on the FS, and \bar{v}_F and \bar{N}_F are the average Fermi velocity and average DOS at the FS. For a circular FS, $v_F(\mathbf{k}) = \bar{v}_F = v_F$ and $\bar{N}_F = N_F$, but the approach also holds for lattice models of fermionic dispersion.

Since $\gamma^{(a)}(\mathbf{k}, \mathbf{p})$ is a real, symmetric matrix, it has a complete set of eigenstates $\phi_{\mathbf{k}}^{(a,l)}$ and eigenvalues $\lambda^{(a,l)}$:

$$\sum_{\mathbf{p}} \gamma^{(a)}(\mathbf{k}, \mathbf{p}) \phi_{\mathbf{p}}^{(a,l)} = \lambda^{(a,l)} \phi_{\mathbf{k}}^{(a,l)}. \quad (3)$$

Since all the systems we will consider are inversion symmetric, the spin symmetry is implicitly determined by whether l transforms under an irreducible representation that is even or odd under inversion, so we will henceforth leave it implicit, $(a,l) \rightarrow (l)$. Among all the possible solutions, we identify the most negative eigenvalue,

$$\lambda \equiv \text{Min}[\lambda^{(l)}], \quad \lambda < 0. \quad (4)$$

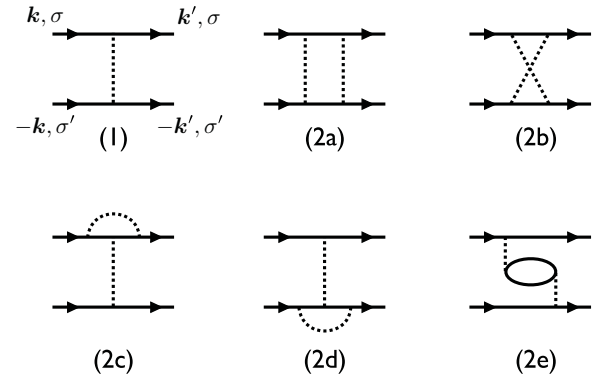


FIG. 1. First- and second-order diagrams which contribute to the effective interaction $\Gamma^a(\mathbf{k}, \mathbf{p})$ in the Cooper channel. The solid line corresponds to an electron propagator whereas the dashed line represents an interaction vertex; σ and σ' are spin indices. The singlet and triplet components $\Gamma^{(s)}$ and $\Gamma^{(t)}$ are obtained by antisymmetrizing the interaction and taking symmetric and antisymmetric combinations, $[\Gamma(\mathbf{k}, \mathbf{p}) + \Gamma^a(\mathbf{k}, -\mathbf{p})]/2$ and $[\Gamma(\mathbf{k}, \mathbf{p}) - \Gamma^a(\mathbf{k}, -\mathbf{p})]/2$, respectively.

Then,

$$T_c \sim E_F \exp[-1/|\lambda|]. \quad (5)$$

Since the effective interaction Γ is computed perturbatively assuming weak interactions, λ can be expressed as a power series in the bare interaction. Assuming that the interaction is a local Hubbard U , we have

$$\lambda = -|u|[1 + a_1|u| + a_2u^2 + \dots] \quad (6)$$

for negative U ($u = N_F U$) and

$$\lambda = -u^2[b_0 + b_1u + b_2u^2 + \dots] \quad (7)$$

for positive U . a_i and b_i are nonuniversal constants which depend on dimensionality, crystalline point group, electron concentration, and details of the band structure. The absence of a linear in u term in λ for $U > 0$ is a consequence of the fact that in a repulsive Hubbard model, an attractive interaction in any pairing channel can only appear due to a renormalization of the original interaction by the particle-hole continuum. As a consequence, T_c is a highly nonanalytic function of u in the limit $u \rightarrow 0$, with different functional dependencies for positive and negative u .

In the next two sections we apply this general procedure to systems with isotropic dispersion, and to systems with full lattice dispersion.

III. CONTINUUM ELECTRONS WITH WEAK SHORT-RANGED INTERACTIONS

Dilute electrons on a lattice treated in the effective mass approximation are equivalent to the continuum problem in which the FS is a sphere (a circle in 2D) and the electronic dispersion has the parabolic form $\epsilon_k = k^2/2m - \mu$. As a first example, we thus consider the low-density limit of electrons with an interaction $U(r)$ of finite range r_0 , which is independent of the electron density. There are thus two independent small parameters: $k_F r_0 \ll 1$ and $k_F a \ll 1$, where $a \equiv m\tilde{U}(0)/4\pi \sim$

$mU(r=0)r_0^3$ is the s -wave scattering length in the Born approximation and \tilde{U} is the Fourier transform of U .

To first order in U , the singlet and triplet components of the pairing interaction in the momentum space are

$$\begin{aligned}\Gamma^{(s)}(\mathbf{k}, \mathbf{p}) &= [\tilde{U}(\mathbf{k} - \mathbf{p}) + \tilde{U}(\mathbf{k} + \mathbf{p})]/2, \\ \Gamma^{(t)}(\mathbf{k}, \mathbf{p}) &= [\tilde{U}(\mathbf{k} - \mathbf{p}) - \tilde{U}(\mathbf{k} + \mathbf{p})]/2.\end{aligned}\quad (8)$$

For \mathbf{k} and \mathbf{p} located at the FS, $(\mathbf{k} - \mathbf{p})^2 = 2k_F^2(1 - \cos\theta)$. Since $\tilde{U}(\mathbf{k})$ changes slowly over the range of momenta $0 \leq |\mathbf{k}| \leq 2k_F$, it can be expanded in powers of $k_F r_0 \ll 1$:

$$\tilde{U}(\mathbf{k}) = \tilde{U}(0)(1 + \alpha_1 |\mathbf{k}|^2 r_0^2 + \alpha_2 |\mathbf{k}|^4 r_0^4 + \dots), \quad (9)$$

where α_n are pure numbers related to moments of $U(r)$. The first term in Eq. (9) then contributes to s -wave pairing, the second term contributes to s -wave and p -wave pairing, the third term contributes to s -wave, p -wave, and d -wave pairing, and so on. Indeed, because there is full rotational symmetry, the pairing wave functions [i.e., the eigenstates in Eq. (3)] are completely determined by symmetry (i.e., they are uniquely specified by angular momentum sectors labeled by l). Correspondingly, the eigenvalues, $\lambda^{(l)}$, can be computed directly as the appropriate symmetry determined average of γ over the FS. In 3D, $N_F = mk_F/(2\pi^2)$, and it is important to note that $u = N_F \tilde{U}(0) = 2(ak_F)/\pi$.

Then, following the renormalization group procedure outlined above, explicit perturbative expressions can be obtained for $\lambda^{(l)}$ which, to second order in u , are

$$\lambda^{(l)} = (k_F a)A^{(l)} + (k_F a)^2 B^{(l)} + \dots, \quad (10)$$

where $A^{(l)}$ and $B^{(l)}$ are dimensionless functions of the dimensionless variables, $k_F r_0$ and $N_F \Omega_0$ [where Ω_0 is the scale at which the couplings are defined, as discussed above Eq. (1)]. However, we are interested only in their leading behavior for small values of both these parameters. Starting with the first-order terms, $A^{(l)}$ is manifestly independent of $N_F \Omega_0$ but varies as $k_F r_0 \rightarrow 0$ according to $A^{(l)} \sim (k_F r_0)^{2l}$. Specifically, for the three lowest angular momentum channels,

$$\begin{aligned}A^{(s)} &= \frac{2}{\pi}, & A^{(p)} &= -\frac{\alpha_1}{\pi}(r_0 k_F)^2, \\ A^{(d)} &= \frac{\alpha_2}{\pi}(r_0 k_F)^4.\end{aligned}\quad (11)$$

The components with larger l are progressively smaller in powers of $r_0 k_F$. To this order, the sign of $\lambda^{(l)}$ depends on the sign of a and on the sign of α_l . For a repulsive Yukawa potential (i.e., for $\tilde{U}(q) = \tilde{U}(0)/[1 + (qr_0)^2]$), $a > 0$, $\alpha_1 < 0$, and $\alpha_2 > 0$, and this is rather generic for purely repulsive interactions. Thus, there is no Cooper instability to first order in $(k_F a)$.

The situation is altered by corrections to $\Gamma^{(a)}(\mathbf{k}, \mathbf{p})$ to second order in ak_F ; see Fig. 1. The diagram 2a in the figure describes the renormalization in the particle-particle channel which makes a contribution to $B^{(s)}$ in the s -wave channel proportional to $\ln[W/\Omega_0]$. However, so long as the inequality in Eq. (1) is satisfied, this only produces a small correction to $\lambda^{(s)}$ relative to the first-order repulsive term. The other four second-order diagrams which contribute to $B^{(l)}$ contain particle-hole bubbles and account for the important renormalizations of the irreducible pairing interaction.

A key result obtained already by KL (Ref. 1) is that, as $k_F r_0 \rightarrow 0$, $B^{(l)} \rightarrow \beta_l \neq 0$. KL further showed that for sufficiently large $l > 0$, $B^{(l)}$ are negative, and that while $A^{(l)}$ falls exponentially with increasing l , $B^{(l)} \sim l^{-4}$. From this, they concluded that superconductivity in some (possibly high l) channel was inevitable.

We focus attention on the physically more important cases of relatively small l . It has been shown^{2,3} that β_l are negative for $l > 0$. As a result,

$$\pi\lambda^{(p)} = (ak_F)[|\alpha_1|(r_0 k_F)^2 - |\beta_1|(ak_F) + O(k_F a)^2], \quad (12)$$

$$\pi\lambda^{(d)} = (ak_F)[|\alpha_2|(r_0 k_F)^4 - |\beta_2|(ak_F) + \dots],$$

where all β_l are of order 1. The issue then is which terms are larger, the negative second-order or the positive first-order contributions. Clearly for $k_F^{-1} \gg r_0 \gg a$, the repulsive part of the interaction is dominant. However, there is a broad range of circumstances in which $k_F^{-1} \gg r_0 \sim a$. In this situation, the attractive interactions dominate, even for relatively small $l > 0$. In 3D

$$\beta_1 = -\frac{8(2 \log 2 - 1)}{5\pi^2}, \quad \beta_2 \sim 10^{-2}\beta_1 \quad (13)$$

(see Refs. 2,3), and hence at small density a 3D Fermi system with short-range repulsive interactions undergoes a p -wave pairing transition with

$$T_c \propto \exp\{-1/[|\beta_1|(ak_F)^2]\}. \quad (14)$$

(For the full calculation of T_c see Ref. 35.) In 2D, the calculations are a bit more tricky because the static particle-hole bubble for free fermions is independent of momentum transfer for $|\mathbf{k} - \mathbf{p}| < 2k_F$, so one has to go to the next, third order, to obtain the momentum dependence of the dressed interaction (see Ref. 7). The final result is, however, similar to the one in 3D: A 2D Fermi system at a small density undergoes a p -wave superconductivity with a low T_c .

Note that a similar analysis was carried out in Ref. 36 for the extended Hubbard model at small electron densities, where instead of a Yukawa interaction, strong Hubbard interactions were considered with $U \gg V \gg$ the bandwidth with similar results to those discussed here.

IV. EXTENDED HUBBARD MODEL AT WEAK COUPLING

As a second more directly experimentally relevant example, we apply the reasoning from Sec. II to a higher density of electrons in the extended Hubbard model on a two-dimensional square lattice with the Hamiltonian

$$\begin{aligned}H &= H_0 + H_{\text{int}}, \\ H_0 &= -t \sum_{\langle ij \rangle \sigma} c_{i\sigma}^\dagger c_{j\sigma} + \text{H.c.}, \\ H_{\text{int}} &= U \sum_i n_{i\uparrow} n_{i\downarrow} + V \sum_{\langle i,j \rangle} n_i n_j + V' \sum_{\langle\langle i,j \rangle\rangle} n_i n_j,\end{aligned}\quad (15)$$

where $c_{i\sigma}$ is the destruction operator of an electron on lattice site i , with spin σ ; $\langle i, j \rangle$ and $\langle\langle i, j \rangle\rangle$ denote nearest-neighbor and second-neighbor pairs of sites respectively; $n_i = \sum_\sigma c_{i\sigma}^\dagger c_{i\sigma}$ and the average density of electrons per site is $n \equiv \langle n_i \rangle$. For simplicity, we consider band electrons with only

nearest-neighbor hopping. As is well known, such a system possesses a nongeneric particle-hole symmetry. This feature, however, does not play a significant role in the resulting phase diagram since we consider the model away from half filling. (See, however, Ref. 37.)

To begin with, for $V' = 0$ we show that the phase diagram is drastically different depending on the ratio V/U , even as $u \sim U/t \rightarrow 0$. Different asymptotic analysis is required for the case $V = \alpha U^2/W$ (i.e., for $u \rightarrow 0$ with $VW/U^2 = \alpha > 0$ held constant), and $V = \alpha' U$ (i.e., for $u \rightarrow 0$ with $V/U = \alpha' > 0$ held fixed). We find that in both cases, the ground state is superconducting for all dopings, but the symmetry of the pairing state is generally different. We then add $V' \sim V$ and show that it adds other pairing states to the phase diagram.

A. $V \sim U^2/W$, $V' = 0$

Since the effective interaction is computed to $O(U^2)$, when $V = \alpha U^2/W$, we only need take V into account to first order (diagram 1 in Fig. 1), i.e., at the bare level. A nonzero V then produces a correction to the effective $\Gamma(\mathbf{k}, \mathbf{p})$ in the form

$$\begin{aligned} \delta\Gamma(\mathbf{k}, \mathbf{p}) &= \alpha \frac{U^2}{W} [\cos(k_x - p_x) + \cos(k_y - p_y)] \\ &= \alpha \frac{U^2}{W} \sum'_{(\eta)} \phi^{(\eta,1)}(\mathbf{k}) \phi^{(\eta,1)}(\mathbf{p}), \end{aligned} \quad (17)$$

where in the second line the sum is taken over appropriate basis functions defined on nearest-neighbor sites with A_{1g} or extended s -wave symmetry, B_{1g} or $d_{x^2-y^2}$ -wave symmetry, and E_u or p -wave symmetry:

$$\begin{aligned} A_{1g} : \phi^{(s,1)}(\mathbf{k}) &= [\cos(k_x) + \cos(k_y)]/\sqrt{2}, \\ B_{1g} : \phi^{(x^2-y^2,1)}(\mathbf{k}) &= [\cos(k_x) - \cos(k_y)]/\sqrt{2}, \\ E_u : \phi^{(x,1)}(\mathbf{k}) &= \sin(k_x), \quad \phi^{(y,1)}(\mathbf{k}) = \sin(k_y). \end{aligned} \quad (18)$$

Thus, the nearest-neighbor interaction acts as a separable repulsive interaction within these subspaces. Because all three components are repulsive, V tends to suppress the pairing tendency in all three of these channels. However, note that unlike the case in the continuum, there are multiple (infinite) orthogonal functions defined on the FS which transform according to each irreducible representation of the point group—for instance $\phi^{(s,2)} \sim [\cos(k_x) + \cos(k_y)]^2$ also transforms according to A_{1g} under operations of the point group. Thus, even for large α , the presence of a repulsive first-order term in a given channel does not preclude the existence of a more “extended” form of pairing in the same channel.

It has been shown previously in various studies of the repulsive U Hubbard model that near half filling,^{5,8,29,37} predominant pairing instability to order U^2 is in the $d_{x^2-y^2}$ channel, and the subdominant pairing eigenvalue occurs in the A_{2g} or g -wave channel, while somewhat further from half filling, at $n < 0.62$, there is a range of electron concentrations for which the B_{2g} or d_{xy} pairing solution is dominant: Representative gap functions (of the shortest possible spatial range) with these symmetries are

$$\begin{aligned} \phi^{(g,3)} &\sim [\cos(k_x) - \cos(k_y)] \sin(k_x) \sin(k_y), \\ \phi^{(xy,2)} &\sim \sin(k_x) \sin(k_y). \end{aligned} \quad (19)$$

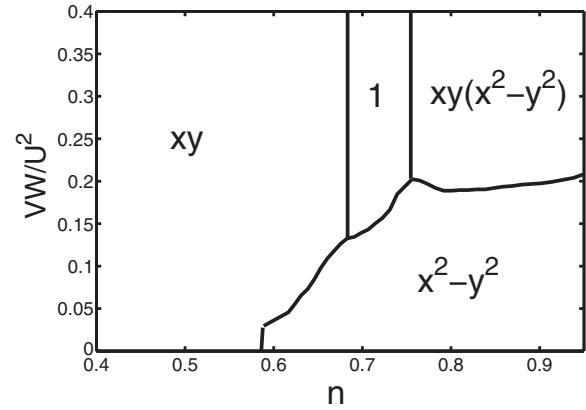


FIG. 2. Phase diagram as a function of electron concentration for the 2D extended Hubbard model in the regime where $V \sim U^2/W$ and $V' = 0$. The region of extended s -wave superconductivity is labeled as 1. For $V = 0$, our phase diagram is similar but not identical to the one obtained by Hlubina (Ref. 5). In his calculation, there is a small region of p -wave superconductivity between the d_{xy} and $d_{x^2-y^2}$ phases. We found only d -wave states.

Figure 2 shows the phase diagram to order U^2 , which we obtained numerically for $V = \alpha U^2/W$, as a function of α and n . Since the analysis considered here breaks down for concentrations sufficiently close to half filling because of competition with antiferromagnetism, we have investigated solutions only for $0 < n < 0.95$. For $0.76 < n < 0.95$, a finite $\alpha \geq 0.2$ destabilizes the $d_{x^2-y^2}$ solution in favor of the subdominant g -wave solution [labeled as $xy(x^2 - y^2)$ on the phase diagram in Fig. 2]. For $0.68 < n < 0.76$ a finite α again destabilizes the $d_{x^2-y^2}$ solution, but the state that emerges instead has a particular extended s -wave symmetry, which is dominantly of the form $\text{Re}(x + iy)^4$. To shorten notations, we have labeled it as “1”.

This state has zero amplitude for on-site pairing in this limit but transforms nevertheless as a trivial irreducible representation of the tetragonal point group. Note that since the g -wave state is $\text{Im}(x + iy)^4$, in the continuum limit, the “1” and g states are degenerate corresponding to angular momentum $\ell = 4$ pairing. However, lattice effects lift this degeneracy. Indeed, there is a phase transition between the g -wave and extended s -wave state at $n = 0.76$, which reflects a level crossing of these two eigenvalues, both of which are subleading at $V = 0$. Note that this phase boundary is vertical since the two solutions are unaffected by V to first order. For $0.58 < n < 0.68$, we have found that a finite α favors the d_{xy} solution. The phase boundary between d_{xy} and extended s -wave phases is also vertical.

B. $V \sim U^2/W$, $V' \sim V$

Next, we consider the effect of a nonzero second-neighbor interaction V' on the phase diagram. Specifically, we take $V' = \alpha_2 V$, $0 < \alpha_2 < 1$. In this case, $V' \sim U^2/W$, so like V , its effects can be computed via the first-order diagram 1 in Fig. 1. The expansion of the V' interaction into angular harmonics is straightforward, and in addition to terms already present in

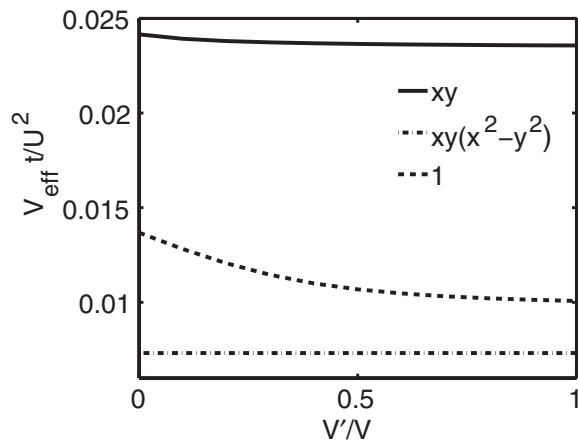


FIG. 3. The effective interaction $V_{\text{eff}} = \lambda/N_F$, where N_F is the density of states at the Fermi level, as a function of $V'/V = \alpha_2$. $n = 0.6$ with $V = \alpha U^2/W$, $\alpha = 0.16$, and nonzero V' .

Eq. (17), one finds the following contribution to the effective Cooper channel interaction from V' :

$$\delta\Gamma_{V'}(\mathbf{k}, \mathbf{p}) = 2\alpha\alpha_2 \frac{U^2}{W} \cos(k_x - p_x) \cos(k_y - p_y). \quad (20)$$

This term is a sum of separable repulsive interactions in the extended s - (A_{1g}), d_{xy} - (B_{2g}), and p -wave (E_u) subspaces. It is important to stress that it does not affect the $d_{x^2-y^2}$ - (B_{1g}) or the g -wave (A_{2g}) subspaces. Thus, relatively close to half filling where the leading eigenvalues belong to the $d_{x^2-y^2}$ - and g -wave subspaces, the phase boundaries are unaffected by V' . We have studied the phase diagram in the presence of nonzero V' and have found that while the phase boundaries are affected quantitatively by nonzero α_2 , the topology of the phase diagram itself is unchanged. We have observed that the pairing strengths are surprisingly robust in this regime, as α_2 is increased. Figure 3 displays the effective interactions $V_{\text{eff}} = |\lambda|/N_F$, where N_F is the density of states at the Fermi energy, in the presence of nonzero V' . For definiteness, we work in a fixed density of electrons $n = 0.6$ and fixed $\alpha = 0.16$ and show the effective interaction as a function of α_2 . The $d_{x^2-y^2}$ pairing strength is the weakest one here and is not shown. It is apparent from the figure that while the pairing strengths of the d_{xy} - and extended s -wave states are affected by nonzero α_2 , this repulsion is not strong enough to suppress superconductivity altogether.

C. $V \sim U$

Next, we consider the case when $V \sim U$, in which case the bare repulsive interactions are of the form

$$\Gamma_I(\mathbf{k}, \mathbf{k}') = U + Vg(\mathbf{k} - \mathbf{k}'), \quad (21)$$

where the subscript on Γ above is to remind the reader that this comes from diagram I in Fig. 1. The dimensionless function

$$g(\mathbf{q}) = \cos q_x + \cos q_y + 2\beta \cos q_x \cos q_y \quad (22)$$

specifies the momentum dependence of the interactions, where $\beta = V'/V$. We must now compute the perturbation expansion of the effective interaction in the Cooper channel to second

order in all the bare interactions, which has the form

$$\Gamma^{(s)}(\mathbf{k}, \mathbf{k}') = \Gamma_I(\mathbf{k}, \mathbf{k}') + U^2 f_1^{(s)}(\mathbf{k}, \mathbf{k}') + V^2 f_2^{(s)}(\mathbf{k}, \mathbf{k}') + UV f_3^{(s)}(\mathbf{k}, \mathbf{k}') + \dots, \quad (23)$$

where s denotes the spin-singlet channel. It is straightforward to show that

$$f_1^{(s)}(\mathbf{k}, \mathbf{k}') = N_F \ln \left[\frac{W}{\Omega_0} \right] + \chi(\mathbf{k} + \mathbf{k}') + O(\Omega_0), \quad (24)$$

where N_F is the density of states at the Fermi energy. The first term is obtained from diagram 2a and the second from 2b in Fig. 1. Similarly,

$$f_2^{(s)}(\mathbf{k}, \mathbf{k}') = N_F (g \star g)(\mathbf{k} - \mathbf{k}') \ln \left[\frac{W}{\Omega_0} \right] + \chi_1(\mathbf{k}, \mathbf{k}') + g(\mathbf{k} - \mathbf{k}') \chi_2(\mathbf{k}, \mathbf{k}') - 2[g(\mathbf{k} - \mathbf{k}')]^2 \chi(\mathbf{k} - \mathbf{k}') + O(\Omega_0), \quad (25)$$

where the first term comes from diagram 2a, the second from 2b, the third from 2c and 2d, and the last term from 2e in Fig. 1. The convolution that enters in the first term is found to be [assuming that the FS averages $\langle \cos 2l_x \rangle = \langle \cos 2l_y \rangle = 0$, where \mathbf{l} and $-\mathbf{l}$ are intermediate fermionic momenta in Fig. 1(a)]

$$(g \star g)(\mathbf{q}) = \frac{1}{2}(\cos q_x + \cos q_y) + \beta^2 \cos q_x \cos q_y. \quad (26)$$

Lastly,

$$f_3^{(s)}(\mathbf{k}, \mathbf{k}') = a N_F g(\mathbf{k} - \mathbf{k}') \ln \left[\frac{W}{\Omega_0} \right] + \chi_2(-\mathbf{k}, \mathbf{k}') + \chi_2(\mathbf{k}, \mathbf{k}') + 2g(\mathbf{k} - \mathbf{k}') \chi(\mathbf{k} - \mathbf{k}') + O(\Omega_0), \quad (27)$$

where a is a constant of order unity. The first term is obtained from diagram 2a, the second from 2b, the third from 2c, and the last from 2e in Fig. 1. The functions $\chi(\mathbf{q})$, $\chi_1(\mathbf{k}, \mathbf{k}')$, and $\chi_2(\mathbf{k}, \mathbf{k}')$ are generalized susceptibilities and are all expressible in terms of the one-electron Matsubara Green's function, $G(p) = (i\omega_p - \epsilon_p)^{-1}$:

$$\begin{aligned} \chi(\mathbf{q}) &= \int_p G(p)G(p+q), \quad \int_p \equiv \int \frac{d^d p d\omega_p}{(2\pi)^{d+1}}, \\ \chi_1(\mathbf{k}, \mathbf{k}') &= \int_p g(\mathbf{k} - \mathbf{p})g(\mathbf{p} - \mathbf{k}')G(p)G(p - \mathbf{k} - \mathbf{k}'), \\ \chi_2(\mathbf{k}, \mathbf{k}') &= \int_p [g(\mathbf{p} + \mathbf{k}) + g(\mathbf{p} - \mathbf{k}')] \\ &\quad \times G(p)G(p + \mathbf{k} - \mathbf{k}'). \end{aligned} \quad (28)$$

Similarly, in the spin-triplet channel, the effective interaction takes the form

$$\Gamma^{(t)}(\mathbf{k}, \mathbf{k}') = Vg(\mathbf{k} - \mathbf{k}') + U^2 f_1^{(t)}(\mathbf{k}, \mathbf{k}') + V^2 f_2^{(t)}(\mathbf{k}, \mathbf{k}') + UV f_3^{(t)}(\mathbf{k}, \mathbf{k}') + \dots, \quad (29)$$

where

$$\begin{aligned} f_1^{(t)}(\mathbf{k}, \mathbf{k}') &= -\chi(\mathbf{k} - \mathbf{k}'), \\ f_2^{(t)}(\mathbf{k}, \mathbf{k}') &= f_2^{(s)}(\mathbf{k}, \mathbf{k}'), \\ f_3^{(t)}(\mathbf{k}, \mathbf{k}') &= -2g(\mathbf{k} - \mathbf{k}')\chi(\mathbf{k} - \mathbf{k}'). \end{aligned} \quad (30)$$

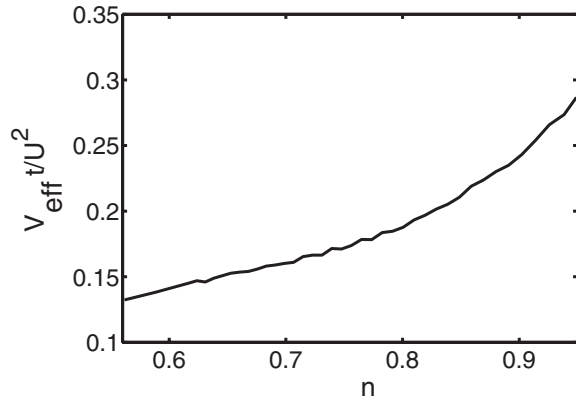


FIG. 4. The effective interaction $V_{\text{eff}} = \lambda/N_F$ for the g -wave state. Here, we have chosen $V = 0.5U$ and $V' = 0.5V$. All other eigenvalues are subdominant and are not shown here.

When $\beta = 0$, the contribution from diagram 2a disfavors solutions which involve nearest-neighbor pairing. For a nonzero β , solutions with second-neighbor pairing amplitude are also suppressed.

In Fig. 4, we show the pairing strength of the A_{2g} (g -wave) state when $V = 0.5U$, $V' = 0.5V$. We have found that the pairing strengths in other channels are significantly weaker and are therefore not shown in the figure. We note that, interestingly, the g -wave pairing strength is much greater in the regime $V \sim U$ since it gains energy from the attractive effective interactions that are obtained at $O(V^2)$, which were neglected in the regime where $V \sim U^2$. Thus, while the states with nearest-neighbor pairing are severely suppressed by momentum dependence of the first-order terms, states involving further ranged pairing are more enhanced by second-order, KL contributions than they are suppressed by first-order contributions. It is important to stress that in the weak-coupling limit, such enhancements cannot be ascribed to a well-defined bosonic “glue,” such as those associated with proximate spin or charge density states, since instabilities toward spin- and charge-ordered phases occur at weak coupling only in exponentially narrow regions in parameter space (close to a perfectly nested Fermi surface, for instance).

V. CONTINUUM ELECTRONS WITH SCREENED COULOMB INTERACTIONS

The Coulomb interaction is long ranged, and so never can be safely treated in perturbation theory. Physically, in a good metal, it should be screened, and so equivalent to an appropriate finite-range model, but because screening at long distances involves electrons with energies arbitrarily close to the Fermi energy, this is something that is subtle to treat in a controlled RG. Simply to replace the Coulomb interaction with a screened Coulomb interaction, and then to carry out the usual RG from there, risks double-counting of certain important physical processes, which are already implicit in the screened form of the interaction. Thus, to treat the Coulomb problem, we are forced to adopt a more qualitative, although still physically sensible, approach, in lieu of the asymptotically exact approach we have pursued up until this section. For simplicity, we again

consider the explicit case of dilute electrons, in which the dispersion is quadratic. It is important to note, however, that for small r_s , where the weak-coupling intuition is most likely to be correct, the screening length is parametrically larger than k_F^{-1} , so even the screened interaction is not, in any naive sense, short ranged.^{29,38}

In 3D, the screened Coulomb interaction within the RPA approximation is

$$\tilde{U}(q) = \frac{4\pi e^2}{q^2 + \kappa^2 \Pi(q)}, \quad (31)$$

where

$$\Pi(q) = \frac{1}{2} + \frac{4k_F^2 - q^2}{8k_F q} \ln \frac{2k_F + q}{2k_F - q}, \quad (32)$$

$\kappa = 0.81k_F r_s^{1/2}$, and $r_s = 1.92e^2/\hbar v_F$. If we calculate the s -wave scattering length and the range of the interaction, as we did in Sec. III, then $ak_F = me^2 k_F/\kappa^2 \approx 0.8$ and $r_0 \sim 1/\kappa \sim a/(r_s)^{1/2}$, so in the “weakly interacting limit” $r_s \ll 1$, it follows that $r_0 \gg a$. Because $ak_F = O(1)$, an expansion in powers of the interaction is not possible. In addition, the screening of the Coulomb interaction already contains one of the diagrams (a particle-hole bubble) which for short-range interactions participated in the KL renormalization of the irreducible pairing interaction. Nonetheless, it is still plausible that the same sort of KL calculation (with the screening diagram omitted) will still give a physically reasonable account of the pairing in this case, although the formal justification for this approach is on somewhat less secure footing.

A. $r_s \ll 1$

For $r_s \ll 1$, since the relevant values of the momentum transfer which enter the various calculations is $|\mathbf{q}| \sim \kappa \ll k_F$, $\tilde{U}(q)$ can be well approximated by taking $\Pi(q) \approx \Pi(0) = 1$. Then

$$\tilde{U}(q) = \frac{4\pi e^2}{q^2 + \kappa^2} \quad (33)$$

and consequently

$$N_F \tilde{U}(q) = 0.041 \frac{r_s}{1 - \cos \theta + 0.164r_s}, \quad (34)$$

where $q = \sqrt{2k_F^2[1 - \cos(\theta)]}$. Expanding this bare $\tilde{U}(q)$ in angular harmonics one finds that they are all positive (repulsive), but that their magnitudes decay with increasing l , eventually as $e^{-lr_s^{1/2}}$ for $lr_s^{1/2} \gg 1$ (Ref. 38).

The KL-type contributions to $\lambda^{(l)}$ come from particle-hole renormalizations which involve particle-hole bubbles (diagrams 2b, 2c, and 2d in Fig. 1). For $l \geq 1$, typical momenta associated with these bubbles are of order k_F , and since $N_F \tilde{U}(k_F) = O(r_s) \ll 1$, this implies that these terms make contributions to $\lambda^{(l)}$ which are small compared to the scale of the repulsive contributions $\sim N_F \tilde{U}(0) = O(1)$. Obviously then, for l not too large, $\lambda^{(l)} > 0$; i.e., there is no superconductivity. The situation is different for large $l > 1/r_s^{1/2}$ owing to the fact that the exchange diagram (diagram 2b in Fig. 1) has a nonanalytic dependence on θ near $\theta = 0$, i.e., when \mathbf{k} and \mathbf{p} are nearly parallel. Moreover, under these circumstances, the typical internal momenta in the particle-hole ladder are

also nearly parallel to \mathbf{k} and \mathbf{p} , from which it follows that the relevant interactions involve near-zero momentum transfer where the interactions are strong, $N_F \tilde{U}(0) = O(1)$ (Ref. 39). Because of this small θ nonanalyticity, the contribution to $\lambda^{(l)}$ from the exchange diagram scales as $1/l^4$ rather than exponentially in l , and so makes the dominant contribution to $\lambda^{(l)}$ for large enough l . This nonanalytic contribution is attractively independent of the parity of l (Ref. 1). Of course, T_c is always very small for such high l pairing, but these arguments suggest that KL-type superconductivity survives.

B. $r_{wc} > r_s > 1$

For $r_s \gg 1$, even in the continuum, electrons form a Wigner crystal state, which is manifestly neither a Fermi liquid nor a superconductor. However, since the critical value r_{wc} for Wigner crystallization appears to be numerically large, it is reasonable to wonder what happens when r_s is in the range $1 < r_s < r_{wc}$. In this range, there is no guarantee that the Fermi-liquid fixed point is even a correct starting point for examining the problem—there could be a variety of possible other phases, and, even if one is prepared to ignore all standards of mathematical rigor, there is no controllable expansion because $N_F \tilde{U}(q)$ is of order one for all q which connect points on the FS.

The approach adopted by AK to address this point was to assume the same perturbative approach that we have outlined for $r_s \ll 1$ can be applied for $r_s > 1$; i.e., the pairing vertex is calculated to second order in the screened Coulomb interaction which is taken to have the Yukawa form as in Eq. (33), and only the exchange diagram 2e from Fig. 1 is evaluated to determine the second-order contribution to the pairing vertex.

Evaluating $\lambda^{(l)}$ for the first few angular harmonics, one then finds²⁹ that the interactions in the p - and d -wave channels (among others) are repulsive for $r_s \sim 1$, and only become attractive again for unphysically large values, i.e., $r_s > 54$ for p -wave and $r_s > 26.5$ for d -wave pairing. From this AK concluded that the KL mechanism is not a plausible mechanism of superconductivity in systems with Coulomb interactions with $r_s \sim 1$ or greater.

Given that even the starting expression for the screened Coulomb interaction in Eq. (31) makes little sense in the large r_s limit, where the Thomas-Fermi screening length is parametrically smaller than the distance between electrons, it is difficult to judge the validity of this conclusion. We could, with no less justification, repeat the AK calculation but keeping the full RPA expression for the screened Coulomb interaction, Eq. (31), rather than the Yukawa form in Eq. (33). In this case, an attractive pairing vertex is obtained already in first order. (Second-order contributions from diagrams 2b–2d in Fig. 1 would further enhance the pairing tendencies.) As was shown in Ref. 38, the largest attractive pairing component is $l = 1$ for which $\lambda(l = 1) \approx -0.07$.

A very similar $\lambda(l = 1) = 0.06$ has been obtained in Ref. 45. There the full quasiparticle scattering amplitude has been calculated from the coupled Bethe-Salpeter equations for the two particle-hole channels, modeling the irreducible vertex function by comparison with Green's function Monte Carlo data on the charge and spin susceptibilities. The pairing

was found in large part to be due to exchange of transverse current fluctuations.

In the absence of a justified theoretical computational scheme, it is difficult to gauge which approach is better. It is likely that p -wave is the leading attractive pairing component at $r_s \gg 1$ but at which r_s it prevails and what is T_c are the two issues not settled yet.

There are other issues in the large r_s limit. Due to the proximity of the Wigner crystal, the effective interactions are strongly momentum dependent. Magnetically ordered states are also natural in this limit, and proximity to them can give rise to structure in the pairing vertex related to magnetic fluctuations: This observation underlies theories of p -wave pairing near a ferromagnetic³¹ and d -wave pairing near an antiferromagnetic instability.³² However, the quasiparticles themselves may be largely incoherent, making it difficult to know precisely what is being paired. Even if Fermi-liquid theory remains valid, strong forward scattering interactions, which are likely to occur in this limit, can produce large changes in the Fermi-liquid parameters, with major consequences for any theory of superconducting pairing.

VI. DMRG SOLUTION OF EXTENDED HUBBARD LADDERS

To go beyond the weak-coupling limit, where the energy scales associated with superconductivity are exponentially small, one has to resort to numerical methods. In order to address the effect of extended interactions in the intermediate-coupling regime, we have performed DMRG⁴⁰ simulations of the extended Hubbard model [Eq. (15)] on ladders of size $L \times 2$. For $V = V' = 0$, this system is known^{12,41–43} to have a spin gap in the thermodynamic limit when the electron density is close to $n = 1$. The superconducting correlations are d -wave like, in the sense that the pair amplitude has an opposite sign on x - and y -oriented bonds, and falls off with distance as a power law which depends on n and U/t . Here, we examine the sensitivity of the superconducting tendency of the two-leg ladder to adding extended interactions. We do this by calculating the spin gap and the decay of a proximity-induced superconducting order parameter as a function of distance, for various values of V, V' . This study extends earlier results on the t - J model with a nearest-neighbor V ,²⁸ which found that the pairing survives up to $V \approx 4J$.

The spin gap is defined as $\Delta_s = E(S = 1) - E(S = 0)$ where $E(S)$ is the ground-state energy with spin S , extrapolated to the thermodynamic limit $L \rightarrow \infty$, as a function of V . The system sizes used in the extrapolations were $L = 16, 32, 64$. The spin gap is then extrapolated to $L \rightarrow \infty$ by fitting $\Delta_s(1/L)$ to a second-order polynomial. The extrapolated value of Δ_s is up to a factor of 2 smaller than $\Delta_s(L = 64)$; this extrapolation is the largest source of error in our results. The following parameters were used in the calculations: $t = 1$, $U = 8$, $V' = 0$, and $n = 0.875, 0.9375$ (see Fig. 5). As V increases, the spin gap decreases gradually from its $V = 0$ value, but remains finite up to $V \approx 2.5$.

For larger values of V , we observe a transition to a charge density wave (CDW) state, in which there are pronounced oscillations in the electron density at a wave vector close to $\tilde{Q} = (\pi, \pi)$. We have checked that the CDW transition occurs

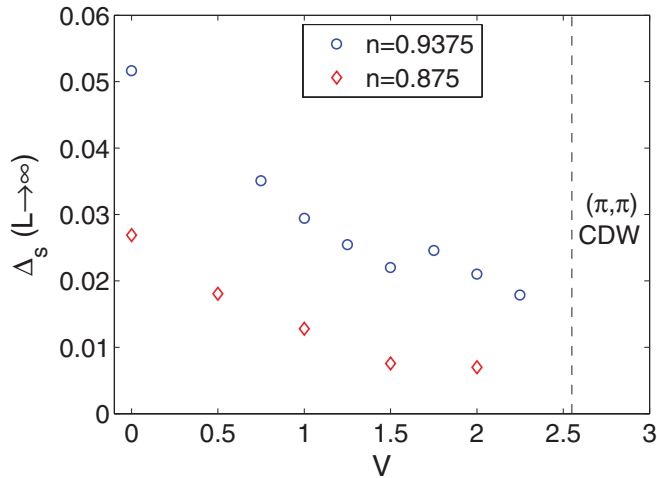


FIG. 5. (Color online) The spin gap Δ_s extrapolated to the thermodynamic limit for two-leg ladders with electron density $n = 0.9375$ (circles) and $n = 0.875$ (diamonds) and $t = 1$, $U = 8$, and $V' = 0$, as a function of V . Beyond $V \approx 2.6$, a transition to a state with pronounced charge density oscillations at a wave vector close to (π, π) is observed.

at $V \approx 2.5$ even for the undoped ($n = 1$) system. The doped CDW state supports gapless spin excitations at the edges, but has a large bulk spin gap $\Delta_s \approx 0.1$. (We infer this by noticing that in the lowest triplet excitation with $S_z = 1$, $\langle S_z \rangle$ is nonzero only close to the edges. We have also computed the gap to an excitation with $S_z = 2$, in which $\langle S_z \rangle$ is nonzero in the bulk, and found that this gap is finite in the thermodynamic limit.)

We have also examined the effect of a second-neighbor V' on the spin gap. Figure 6 shows the spin gap as a function of V' for $V = 1$, $n = 0.9375$. Again, we find that while Δ_s decreases monotonically upon increasing V' , its effect is not dramatic. For example, upon reaching $V' = 0.5t$, Δ_s has decreased to about 50% of its $V = 1$, $V' = 0$ value.

The superconducting response of a ladder system can be characterized by the rate at which an externally induced superconducting order parameter at the edge decays as we move into the bulk. In a gapless one-dimensional system, this amplitude decays as a power law; in a two-leg ladder with a spin gap, this power law can be shown to be equal to $\frac{1}{4K_c}$,⁴⁴ where K_c is the Luttinger parameter of the (gapless) even charge mode. Figure 7 shows the induced order parameter on a y bond,

$$P_y(x) = \frac{1}{2}[c_\uparrow(x,1)c_\downarrow(x,2) - c_\downarrow(x,1)c_\uparrow(x,2)], \quad (35)$$

as a function of position x , on a log-log scale. In this calculation, the following boundary term was added to the Hamiltonian:

$$H_{\text{edge}} = \Delta[c_\uparrow(1,1)c_\downarrow(1,2) - c_\downarrow(1,1)c_\uparrow(1,2) + \text{H.c.}], \quad (36)$$

with $\Delta = 0.25$. This term mimics a proximity-induced gap at the edge due to a nearby bulk superconductor. The results are shown for systems of length $L = 32, 48$, density $n = 0.9375$, and $V = 0, 1, 2.5, 3$.

The induced superconducting order parameter is seen to decrease monotonically upon increasing V . However, the slope of $\ln(|P_y|)$ vs $\ln(x)$ (the power with which the superconducting

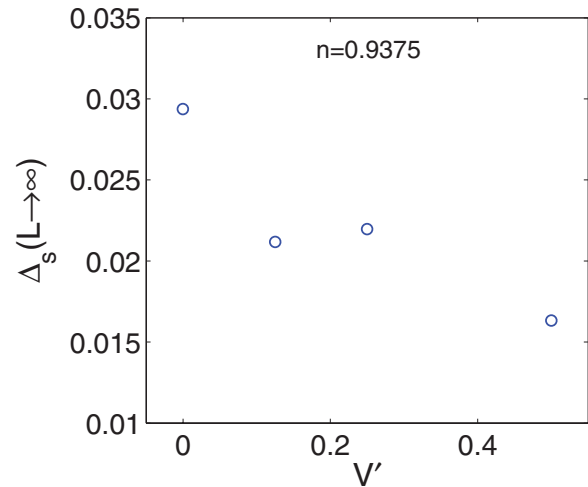


FIG. 6. (Color online) The spin gap $\Delta_s(L \rightarrow \infty)$ as a function of V' for two-leg ladders with $n = 0.9375$, $t = 1$, $U = 8$, and $V = 1$.

order parameter decays) far away from the edge is not strongly dependent on V , except for $V > 2.5$. Although our systems are not long enough to allow an accurate estimate of the slope, one can roughly estimate $K_c \sim 0.4-0.6$, well within the range of divergent superconducting correlations $K_c > 0.25$, and close to the value in which superconducting and CDW correlations decay with the same exponent, $K_c = 0.5$.

The inset of Fig. 7 shows the induced superconducting order parameter on various bonds near the middle of the $L = 48$ system with $V = 1$. As can be seen in the figure, the order parameter is “ $d_{x^2-y^2}$ like,” in the sense that the pairing amplitude on x - and y -oriented bonds is opposite in sign, and the amplitude on the diagonal (next-nearest neighbor) is relatively small. The order parameter has a $d_{x^2-y^2}$ -like structure

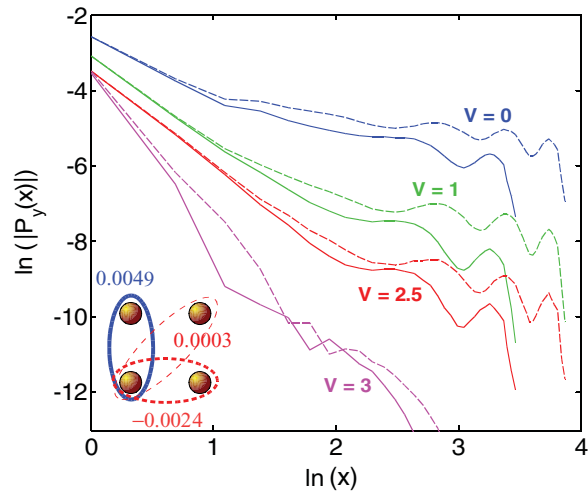


FIG. 7. (Color online) Induced superconducting order parameter as a function of position in a calculation with an edge pair field [Eq. (36)] of magnitude $\Delta = 0.5$. In these calculations, $t = 1$, $U = 8$, $n = 0.9375$. Solid (dashed) lines correspond to $L = 32$ ($L = 48$). Results for $V = 0, 1, 2.5, 3$ are shown. The inset shows the induced order parameter on nearest- and second-nearest-neighbor bonds near the middle of an $L = 48$ system with $V = 1$.

for $0 < V < V_c \approx 2.5$. For larger values of V (in the CDW phase), the order parameter has an extended s -wave structure, in which the pairing amplitude has the same phase on x - and y -oriented bonds. In this regime, however, the order parameter is much smaller than for $V < V_c$ and it decays much faster as a function of distance from the edge (possibly exponentially).

VII. DISCUSSION

In this paper we have shown, using a variety of methods, that unconventional superconductivity arising directly from electron-electron interactions can survive even in the presence of longer (but finite) ranged interactions. First, we have shown that the Kohn-Luttinger effect survives even when the range of the interaction exceeds the s -wave scattering length, provided that the range r_0 satisfies $r_0 \ll k_F^{-1}$. In this regime, the leading instability need not occur for an unphysically high angular momentum and in most cases occurs for $\ell = 1$. For lattice electrons near half filling in the weak-coupling limit, we have found that the $d_{x^2-y^2}$ superconductivity that occurs in the Hubbard model survives in the presence of longer-ranged repulsive interactions V, V', \dots , provided that these interactions are no larger than $\alpha U^2/W$, where α is a constant of order unity. Lastly, we have shown, using DMRG calculations, that in the intermediate-coupling regime, the spin-gap survives even in the presence of a substantial nearest-neighbor interaction, suggesting the stability of $d_{x^2-y^2}$ superconductivity against longer-ranged interactions.

Our findings have possible relevance for understanding some aspects of the effect of material-specific changes in

the electronic structure on the transition temperatures of unconventional superconductors. Although we have shown that unconventional superconductivity from repulsive interactions is a robust phenomenon, which survives in the presence of substantial farther-range repulsions, there is nonetheless a strong tendency for such interactions to produce a significant reduction of T_c . Conversely, if screening by a proximate polarizable medium reduces V and V' , this could lead to a marked enhancement of T_c .

As a point of comparison, recall that in a conventional electron-phonon superconductor, T_c depends on the electron-electron interactions only through μ^* . However, because of retardation, $\mu^* \sim 1/\ln[E_F/\omega_0]$ is largely independent of the bare electron-electron interaction. Moreover, the effective attraction induced by the phonons is typically highly local, and so is also unlikely to be very sensitive to small changes in the environment. Thus, a sensitivity to the screening effects of a polarizable environment may be one of the uniquely characteristic features of pairing due to electron-electron interaction.

ACKNOWLEDGMENTS

We thank A. S. Alexandrov, S. Doniach, T. Geballe, M. Yu. Kagan, and D. J. Scalapino for useful discussions. This work was supported in part by NSF-DMR-0906953 (A.V.C.), DMR-0758356 (S.A.K.), DMR-0757145, DMR-0705472 (E.B.), and startup funds at Stanford University (S.R.). S.R. and A.V.C. also wish to thank the Aspen Center for Physics where part of this work was carried out.

¹W. Kohn and J. M. Luttinger, *Phys. Rev. Lett.* **15**, 524 (1965).

²D. Fay and A. Layzer, *Phys. Rev. Lett.* **20**, 187 (1968).

³M. Yu. Kagan and A. V. Chubukov, *JETP Lett.* **47**, 614 (1988); M. Baranov, A. V. Chubukov, and M. Yu. Kagan, *Int. J. Mod. Phys.* **6**, 2471 (1992).

⁴M. A. Baranov and M. Y. Kagan, *Z. Phys. B* **86**, 237 (1992).

⁵R. Hlubina, *Phys. Rev. B* **59**, 9600 (1999); J. Mráz and R. Hlubina, *ibid.* **67**, 174518 (2003).

⁶A. V. Chubukov and J. P. Lu, *Phys. Rev. B* **46**, 11163 (1992).

⁷A. V. Chubukov, *Phys. Rev. B* **48**, 1097 (1993).

⁸S. Raghu, S. A. Kivelson, and D. J. Scalapino, *Phys. Rev. B* **81**, 224505 (2010).

⁹S. R. White, S. Chakravarty, M. P. Gelfand, and S. A. Kivelson, *Phys. Rev. B* **45**, 5062 (1992); M. Caffarel and W. Krauth, *Phys. Rev. Lett.* **72**, 1545 (1994); D. J. Scalapino and S. A. Trugman, *Philos. Mag. B* **74**, 607 (1996). For the latest developments, see S. Okamoto and T. A. Maier, *Phys. Rev. B* **81**, 214525 (2010), and references therein.

¹⁰T. A. Maier, M. Jarrell, T. C. Schulthess, P. R. C. Kent, and J. B. White, *Phys. Rev. Lett.* **95**, 237001 (2005).

¹¹K. Haule and G. Kotliar, *Phys. Rev. B* **76**, 104509 (2007).

¹²See, e.g., R. M. Noack, S. R. White, and D. J. Scalapino, *Phys. Rev. Lett.* **73**, 882 (1994); *Europhys. Lett.* **30**, 163 (1995); R. M. Noack, N. Bulut, D. J. Scalapino, and M. G. Zacher, *Phys. Rev. B* **56**, 7162 (1997); E. Arrigoni, A. P. Harju, W. Hanke, B. Brendel, and S. A. Kivelson, *ibid.* **65**, 134503 (2002).

¹³G. Karakonstantakis, E. Berg, S. R. White, and S. A. Kivelson, *Phys. Rev. B* **83**, 054508 (2011), and references therein.

¹⁴See, e.g., R. Thomale, C. Platt, J. Hu, C. Honerkamp, and B. A. Bernevig, *Phys. Rev. B* **80**, 180505 (2009); F. Wang, H. Zhai, Y. Ran, A. Vishwanath, and D.-H. Lee, *Phys. Rev. Lett.* **102**, 047005 (2009), and references therein.

¹⁵P. Monthoux and D. J. Scalapino, *Phys. Rev. Lett.* **72**, 1874 (1994); T. Dahm and L. Tewordt, *Phys. Rev. B* **52**, 1297 (1995); D. Manske *et al.*, *ibid.* **67**, 134520 (2003).

¹⁶Ar. Abanov, A. V. Chubukov, and M. R. Norman, *Phys. Rev. B* **78**, 220507 (2008).

¹⁷B. Kyung, J. S. Landry, and A. M. S. Tremblay, *Phys. Rev. B* **68**, 174502 (2003).

¹⁸See, e.g., S. Pathak, V. B. Shenoy, M. Randeria, and N. Trivedi, *Phys. Rev. Lett.* **102**, 027002 (2009), and references therein.

¹⁹G. Kotliar and J. Liu, *Phys. Rev. B* **38**, 5142 (1988).

²⁰P. A. Lee, N. Nagaosa, and X.-G. Wen, *Rev. Mod. Phys.* **78**, 17 (2006).

²¹S. A. Kivelson, I. P. Bindloss, E. Fradkin, V. Oganesyan, J. M. Tranquada, A. Kapitulnik, and C. Howald, *Rev. Mod. Phys.* **75**, 1201 (2003).

²²V. J. Emery and S. A. Kivelson, *Nature (London)* **374**, 434 (1995).

²³See, e.g., D. Senechal and A.-M. S. Tremblay, *Phys. Rev. Lett.* **92**, 126401 (2004); S. S. Kancharla, B. Kyung, D. Senechal, M. Civelli, M. Capone, G. Kotliar, and A.M.S. Tremblay, *Phys. Rev. B* **77**, 184516 (2008).

- ²⁴M. Imada, *Phys. Rev. B* **72**, 075113 (2005).
- ²⁵See, e.g., D. N. Basov and A. V. Chubukov, *Nature Phys.* **7**, 273 (2011), and references therein.
- ²⁶See, e.g., S. R. White, *Phys. Rev. Lett.* **69**, 2863 (1992).
- ²⁷For a $t - t'$ model with $t' \approx -0.3t$ and a nodal k_F at $(0.4\pi, 0.4\pi)$ [see, e.g., A. Kanigel *et al.*, *Phys. Rev. Lett.* **99**, 157001 (2007)], the holelike FS is nearly circular around (π, π) , with $v_F/a \sim 2t$. Note that this v_F is the bare velocity [without the $1/(1 + \lambda)$ factor].
- ²⁸Claudio Gazza, George B. Martins, José Riera, and Elbio Dagotto, *Phys. Rev. B* **59**, R709 (1999).
- ²⁹A. S. Alexandrov and V. V. Kabanov, *Phys. Rev. Lett.* **106**, 136403 (2011).
- ³⁰H. J. Shulz, *Europhys. Lett.* **4**, 609 (1987); A. T. Zheleznyak, V. M. Yakovenko, and I. E. Dzyaloshinskii, *Phys. Rev. B* **55**, 3200 (1997); K. Le Hur and T. M. Rice, *Ann. Phys. (NY)* **324**, 1452 (2009). For recent developments on Kohn-Luttinger type superconductivity in Fe pnictides and in graphene see D. Podolsky, H.-Y. Kee, and Y. B. Kim, *Europhys. Lett.* **88**, 17004 (2009); A. V. Chubukov, *Physica C* **469**, 640 (2009); O. Vafek and L. Wang, *Phys. Rev. B* **84**, 172501 (2011); J. Gonzalez, *ibid.* **78**, 205431 (2008); R. Nandkishore, L. Levitov, and A. Chubukov, e-print [arXiv:1107.1903](https://arxiv.org/abs/1107.1903); M. Kiesel, C. Platt, W. Hanke, D. A. Abanin, and R. Thomale, e-print [arXiv:1109.2953](https://arxiv.org/abs/1109.2953); W.-S. Wang, Y.-Y. Xiang, Q.-H. Wang, F. Wang, F. Yang, and D.-H. Lee, e-print [arXiv:1109.3884](https://arxiv.org/abs/1109.3884).
- ³¹P. Morel and P. W. Anderson, *Phys. Rev.* **125**, 1263 (1962); N. F. Berk and J. R. Schrieffer, *Phys. Rev. Lett.* **17**, 433 (1966); K. Levin and O. T. Valls, *Phys. Rep.* **98**, 1 (1983).
- ³²See, e.g., D. J. Scalapino, E. Loh Jr., and J. E. Hirsch, *Phys. Rev. B* **34**, 8190 (1986); P. Monthoux, A. V. Balatsky, and D. Pines, *Phys. Rev. Lett.* **67**, 3448 (1991).
- ³³R. Shankar, *Rev. Mod. Phys.* **66**, 129 (1994).
- ³⁴J. Polchinski, e-print [arXiv:hep-th/9210046](https://arxiv.org/abs/hep-th/9210046).
- ³⁵D. V. Efremov *et al.*, *Sov. Phys. JETP* **90**, 861 (2000).
- ³⁶M. Yu. Kagan, D. V. Efremov, M. S. Marienko, and V. V. Val'kov, *Pis'ma Zh. Eksp. Teor. Fiz.* **93**, 807 (2011) [*JETP Lett.* **93**, 725 (2011)].
- ³⁷J. Mráz and R. Hlubina, *Phys. Rev. B* **69**, 104501 (2004).
- ³⁸A. V. Chubukov and M. Yu. Kagan, *J. Phys. Condens. Matter* **1**, 3135 (1989).
- ³⁹S. Raghu and S. A. Kivelson, *Phys. Rev. B* **83**, 094518 (2011).
- ⁴⁰S. R. White, *Phys. Rev. Lett.* **69**, 2863 (1992).
- ⁴¹E. Dagotto, J. Riera, and D. Scalapino, *Phys. Rev. B* **45**, 5744 (1992).
- ⁴²E. Dagotto and T. M. Rice, *Science* **271**, 618 (1996).
- ⁴³L. Balents and M. P. A. Fisher, *Phys. Rev. B* **53**, 12133 (1996).
- ⁴⁴E. Berg, S. A. Kivelson, and D. J. Scalapino, *New J. Phys.* **11**, 085007 (2009).
- ⁴⁵S. Kuchenhoff and P. Wölfle, *Phys. Rev. B* **38**, 935 (1988).